



XXVIIth International Conference on Ultrarelativistic Nucleus-Nucleus Collisions
(Quark Matter 2018)

Photon radiation from heavy-ion collisions in the $\sqrt{s_{NN}} = 19 - 200$ GeV regime

Charles Gale^a, Sangyong Jeon^a, Scott McDonald^a, Jean-François Paquet^b, Chun Shen^c

^a*Department of Physics, McGill University, 3600 University Street, Montréal, QC, H3A 2T8, Canada*

^b*Department of Physics, Duke University, Durham, NC 27708, USA*

^c*Department of Physics, Brookhaven National Laboratory, Upton, New York 11973-5000*

Abstract

We present calculations of prompt and thermal photon production in Au-Au collisions at $\sqrt{s_{NN}} = 19 - 200$ GeV. We discuss features of the spacetime profile of the plasma relevant for electromagnetic emission. We highlight how the suppression of prompt photon production at low $\sqrt{s_{NN}}$ can provide a window to measure thermal photons in low collision energies.

Keywords: Electromagnetic radiation, heavy-ion collisions, quark-gluon plasma, RHIC Beam Energy Scan

1. Introduction

The strongly-coupled quark-gluon plasma produced in heavy ion collisions extends approximately 5 to 10 fm in the plane transverse to the beam axis. This volume of the plasma is sufficient to produce a measurable amount of thermal electromagnetic (“black-body”) radiation. On the other hand, the plasma’s dimensions are sufficiently small for this electromagnetic radiation to escape the plasma with negligible rescattering (see Ref. [1] and references therein). This makes photons invaluable probes of entire spacetime dynamics of heavy ion collisions.

In this work we study photon production in Au-Au collisions in the $\sqrt{s_{NN}} = 19 - 200$ GeV collision energy regime. This corresponds to most of the collision energies probed by the RHIC Beam Energy Scan (Phase 1).

2. Evolution of spacetime profile with $\sqrt{s_{NN}}$

The spacetime evolution of the strongly-coupled quark-gluon plasma is described with 3 + 1D relativistic viscous hydrodynamics. The conservation equation for the net baryon density is solved alongside energy-momentum conservation and the Israel-Stewart-type relaxation equation for the shear stress tensor [2]. Energy deposition is performed by adding sources to the conservation equations, as described in

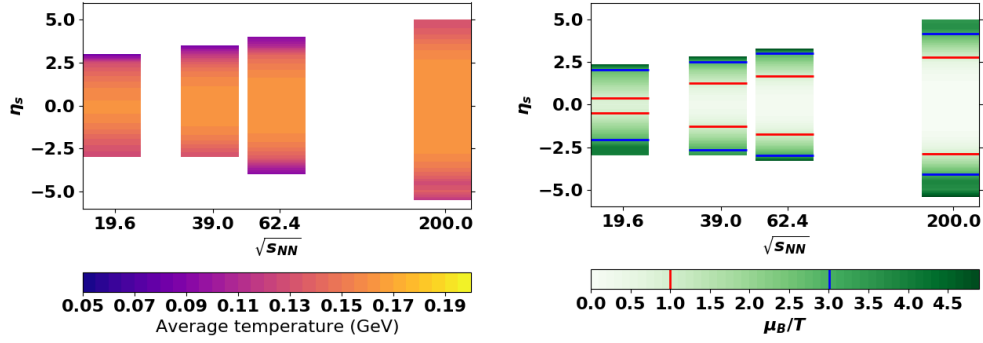


Fig. 1. Average temperature (left) and average μ_B/T (right) as a function of center-of-mass energy $\sqrt{s_{NN}}$ and spatial rapidity η_s for 0 – 5% Au-Au collisions. Markers were added at $\mu_B/T = 1$ (red) and $\mu_B/T = 3$ (blue) on the right-hand plot for reference.

Ref. [3]. This dynamical initialization for the hydrodynamics allows for energy and baryon number to be deposited over an extended period of time, which is the expected scenario in lower energy collisions. A more complete description of the hydrodynamic model can be found in Refs. [4, 5].

At higher collision energies, the baryon current conservation has a relatively small effect on the plasma evolution and can be neglected. In this case the dominant factor determining photon production is the temperature profile of the quark-gluon plasma: how much spacetime volume of plasma is radiating, and what is the temperature distribution of this four-volume. The main difference with lower $\sqrt{s_{NN}}$ collisions is the increasing importance of the baryon chemical potential μ_B , which makes it necessary to account for both the temperature and baryon chemical potential profile.

The evolution of the temperature profile at high collision energies has been investigated in multiple publications (see e.g. Refs. [6, 7, 8]), predominantly in boost-invariant (2 + 1D) calculations that are appropriate for midrapidity observables. In this section we show the dependence of the temperature and baryon chemical potential profile on spatial rapidity of the plasma and on the center-of-mass energy of the collisions. Averages of the temperature and of μ_B/T are calculated and shown as a function of spatial rapidity η_s and center-of-mass energy $\sqrt{s_{NN}}$ in Figure 1.

The averages are computed with the definition $\langle \dots \rangle = \int_{\epsilon(X) > 0.16 \text{ GeV/fm}^3} d^4X \dots / \int_{\epsilon(X) > 0.16 \text{ GeV/fm}^3} d^4X$ with “ \dots ” being either $T(X)$ or $\mu_B(X)/T(X)$. The energy density cut-off $\epsilon(X) > 0.16 \text{ GeV/fm}^3$ corresponds to a temperature of $T=145 \text{ MeV}$ at $\mu_B = 0$. A single event with 0-5% centrality is used for each $\sqrt{s_{NN}}$. Note that the averages are not perfectly symmetrical in spatial rapidity because of physical event-by-event fluctuations in the energy deposition.

Figure 1 summarizes a large amount of information about the space-time profile of the quark-gluon plasma produced in the Beam Energy Scan:

- The temperature and baryon chemical potential vary more slowly around $\eta_s = 0$. At higher collision energies, the $\eta_s = 0$ region forms a well-known plateau extending two to three units of spatial rapidity. This plateau shrinks with decreasing $\sqrt{s_{NN}}$ and essentially vanishes at $\sqrt{s_{NN}} = 19.6 \text{ GeV}$.
- Beyond the central ($\eta_s = 0$) plateau, the average temperature decreases rapidly with spatial rapidity while the ratio μ_B/T increases rapidly.
- The baryon chemical potential at $\eta_s \approx 0$ in $\sqrt{s_{NN}} = 19.6 \text{ GeV}$ collisions corresponds approximately to the baryon chemical potential at $\eta_s \approx \pm 2.5$ in $\sqrt{s_{NN}} = 200 \text{ GeV}$ collisions.

Note that the average temperature in the central plateau ($\eta_s \sim 0$) is not significantly higher at $\sqrt{s_{NN}} = 200 \text{ GeV}$ than it is at $\sqrt{s_{NN}} = 19.6 \text{ GeV}$. The reason for this is in part physical and in part a consequence of the definition of average used in this work. Because the quark-gluon plasma expands rapidly, its low temperature spacetime volume is much larger than its higher temperature volume. This means that averages

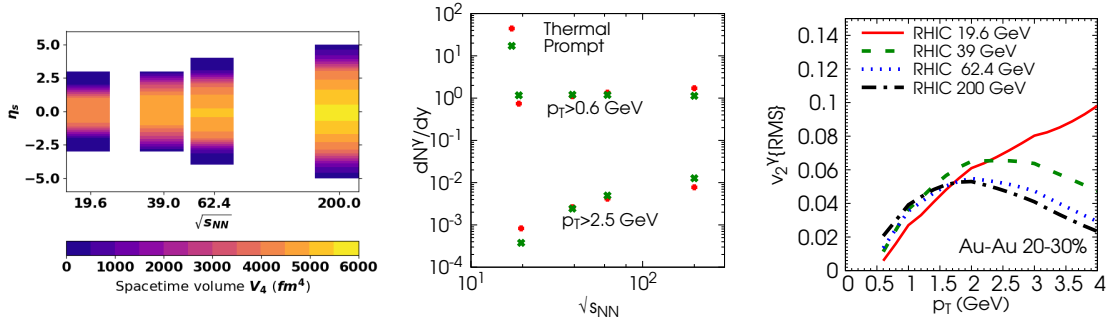


Fig. 2. Left: Spacetime volume of plasma with $\epsilon(X) > 0.16 \text{ GeV}/\text{fm}^3$ as a function of center-of-mass energy $\sqrt{s_{NN}}$ and spatial rapidity η_s . Middle: photon multiplicity at different $\sqrt{s_{NN}}$ with two p_T^γ cuts. Right: Direct photon (thermal + prompt) p_T^γ -differential v_2 coefficient in 20-30% Au+Au collisions at four collision energies.

of temperature tend to be dominated by the lower temperature regions of the plasma no matter what the center-of-mass energy $\sqrt{s_{NN}}$ is. This is a physical effect, and it is known that a large number of photons are produced at lower temperature (late time) by this large spacetime volume. On the other hand, the cut-off used in the average, $\epsilon(X) > 0.16 \text{ GeV}/\text{fm}^3$, excludes very low energy density regions from the average, and thus limits how low the average temperature can be. As long as the cut-off is used consistently across all systems, this is not an issue and different $\sqrt{s_{NN}}$ can still be compared consistently¹.

In Figure 2 (left panel) we show the spacetime volume V_4 of the plasma as defined with the energy density cut-off $\epsilon(X) > 0.16 \text{ GeV}/\text{fm}^3$. Photon emission is only significant in regions where both V_4 and the temperature/ μ_B are large. The rapid decrease of both the spacetime volume and the temperature of radiating plasma as a function of spatial rapidity η_s implies that most photons are produced at $\eta_s \sim 0$, as can be reasonably expected.

3. Photon production in $\sqrt{s_{NN}}$ and momentum rapidity

Thermal photon production is calculated by convoluting the spacetime profile of the medium from hydrodynamics with a photon emission rate calculated from first principles: $k \frac{d^3 N}{d^3 k} = \int d^4 X k \frac{d\Gamma_\gamma}{d^3 k}(T(X), \mu_B(X), \dots)$

The photon emission rate per spacetime volume $k d\Gamma_\gamma/d^3 k$ has been calculated at very high temperature ($\alpha_s(T) \ll 1$) and finite μ_B/T using perturbative QCD in Refs. [9, 10]. The photon rate from an interacting fluid of hadrons at temperatures $T \sim 100 \text{ MeV}$ and $\mu_B/T \sim 0 - 3$ is also known [11, 12]. In this work the photon emission rate of the strongly-coupled quark-gluon plasma is calculated by using this hadronic rate for temperatures below 180 MeV while the perturbative rate is used above this temperature [8]. We expect this prescription to provide a photon emission rate for the strongly-coupled quark-gluon plasma that has a sound temperature and μ_B dependence. We nevertheless emphasize that this prescription should be continuously revisited, both at zero and finite μ_B , as new investigations of the photon emission rates are performed (see Ref. [1] for references to recent works).

Prompt photons are calculated with next-to-leading order perturbative QCD [13] as described in Ref. [8]. We note that we use an extrapolation procedure described in Ref. [8] to obtain prompt photons at low p_T^γ . This extrapolation inevitably introduces a significant uncertainty, especially for low $\sqrt{s_{NN}}$. Given the absence of low p_T^γ p+p photon measurements for most collision energies, we proceed with this extrapolation.

The thermal and prompt photon multiplicity are shown as a function of $\sqrt{s_{NN}}$ on the middle panel of Figure 2. The multiplicity of higher p_T^γ thermal photons ($p_T^\gamma > 2.5 \text{ GeV}$ in this example), which are

¹Temperature averages always require a weight or a cut-off to suppress the contribution of the low temperature regions of the plasma, which essentially extend to infinity. Different prescriptions are used in the literature and comparisons between different results must be made with care.

dominantly produced in higher temperature region of the plasma, increases rapidly with $\sqrt{s_{NN}}$. This can be expected from the increasing volume of high temperature plasma found at higher collision energy. The multiplicity of lower p_T^γ thermal photons ($p_T^\gamma > 0.6$ GeV) increases much more slowly, indicating that there is already a sufficiently large volume of lower temperature plasma to produce thermal photons even in low $\sqrt{s_{NN}}$ collisions.

Interestingly the prompt photon multiplicity at higher p_T^γ increases more rapidly with $\sqrt{s_{NN}}$ than the thermal photon multiplicity. We understand this to be a consequence of suppression of prompt photon production at large values of $x_T^\gamma = 2p_T^\gamma / \sqrt{s_{NN}}$. With $p_T^\gamma \sim 2$ GeV and $\sqrt{s_{NN}} = 19.6$ GeV, $x_T^\gamma \approx 0.2$. It is known that the production of prompt photon decreases more rapidly with x_T^γ when such large values of x_T^γ are probed (see e.g. Ref. [14]). For prompt photon production at lower p_T^γ , our prompt photon multiplicity remains relatively constant with $\sqrt{s_{NN}}$. We believe this is evidence that our calculation of low p_T^γ photons, extrapolated as described in Ref. [8], is being pushed beyond its regime of validity. Low p_T^γ photon measurements in proton-proton collisions will be essential to address this challenge. Nevertheless we believe the rapid change of higher p_T^γ prompt photons with $\sqrt{s_{NN}}$ to be physical in origin, and that it can provide a window into thermal photons in low $\sqrt{s_{NN}}$ collisions.

Finally we show the momentum anisotropy v_2 of photons in the right panel of Fig. 2. The photon v_2 is large at all $\sqrt{s_{NN}}$. The observations of a large v_2 at low $\sqrt{s_{NN}}$ was also made earlier in hadron measurements [15, 16]. With photons, there is however an additional effect not encountered with hadrons: while the *thermal* photon v_2 generally correlates well with the hadronic v_n , the *direct* photon v_2 also incorporates the effect of prompt photons, which suppress the thermal photon v_2 . Since less prompt photons are produced at higher p_T^γ and low $\sqrt{s_{NN}}$ (i.e. large x_T^γ discussed above), the v_2 of direct (thermal+prompt) photon v_2 can reach large values, as observed at high p_T^γ for $\sqrt{s_{NN}} = 19.6$ GeV. While further calculations will be necessary to investigate the effect of viscosity on such high p_T thermal photons, we believe the interesting aspects of photon production at low $\sqrt{s_{NN}}$ supports investing more resources into theoretical and experimental investigations of photon production at low collision energies.

Acknowledgements This work was supported by the U.S. Department of Energy, Office of Science, Office of Nuclear Physics under Award Numbers DE-FG02-05ER41367 (JFP) and de-sc0012704 (CS) and by the Natural Sciences and Engineering Research Council of Canada. CG acknowledges support from the Canada Council for the Arts, through its Killam Research Fellowship Program. SM acknowledges funding from The Fonds de recherche du Québec - Nature et technologies (FRQ-NT) through the Programme de Bourses d'Excellence pour Étudiants Étrangers. Computations were made in part on the supercomputer Guillimin, managed by Calcul Québec and Compute Canada and funded by the Canada Foundation for Innovation (CFI), Ministère de l'Économie, des Sciences et de l'Innovation du Québec (MESI) and FRQ-NT. This research used resources of the National Energy Research Scientific Computing Center, which is supported by the DOE Office of Science under Contract No. DE-AC02-05CH11231.

References

- [1] J.-F. Paquet, J. Phys. Conf. Ser. 832 (1) (2017) 012035.
- [2] G. S. Denicol, C. Gale, S. Jeon, A. Monnai, B. Schenke, C. ShenarXiv:1804.10557.
- [3] C. Shen, B. Schenke, Phys. Rev. C97 (2) (2018) 024907.
- [4] C. Shen, B. Schenke, in: 27th International Conference on Ultrarelativistic Nucleus-Nucleus Collisions (Quark Matter 2018) Venice, Italy, May 14-19, 2018, 2018. arXiv:1807.05141.
- [5] C. Shen, B. Schenke, PoS CPOD2017 (2018) 006.
- [6] R. Chatterjee, H. Holopainen, I. Helenius, T. Renk, K. J. Eskola, Phys. Rev. C88 (2013) 034901.
- [7] C. Shen, U. W. Heinz, J.-F. Paquet, C. Gale, Phys. Rev. C89 (4) (2014) 044910.
- [8] J.-F. Paquet, C. Shen, G. S. Denicol, M. Luzum, B. Schenke, S. Jeon, C. Gale, Phys. Rev. C93 (4) (2016) 044906.
- [9] C. T. Traxler, H. Vija, M. H. Thoma, Phys. Lett. B346 (1995) 329–334.
- [10] H. Gervais, S. Jeon, Phys. Rev. C86 (2012) 034904.
- [11] M. Heffernan, P. Hohler, R. Rapp, Phys. Rev. C91 (2) (2015) 027902.
- [12] S. Turbide, R. Rapp, C. Gale, Phys. Rev. C69 (2004) 014903.
- [13] P. Aurenche, M. Fontannaz, J.-P. Guillet, E. Pilon, M. Werlen, Phys. Rev. D73 (2006) 094007.
- [14] A. Adare, et al., Phys. Rev. D86 (2012) 072008.
- [15] L. Adamczyk, et al., Phys. Rev. C88 (2013) 014902.
- [16] R. Snellings, EPJ Web Conf. 97 (2015) 00025.